STRUCTURAL BIOLOGY COMMUNICATIONS

ISSN 2053-230X

Crystal structure of the ATPase-C domain of the chromatin remodeller Fun30 from *Saccharomyces cerevisiae*

Lan Liu[a,b] and Tao Jiang[a,b]*

[a]National Laboratory of Biomacromolecules, CAS Center for Excellence in Biomacromolecules, Institute of Biophysics, Chinese Academy of Sciences, Datun Road, Chaoyang District, Beijing 100101, People's Republic of China, and [b]University of Chinese Academy of Sciences, Yuquan Road, Beijing 100049, People's Republic of China.
*Correspondence e-mail: tjiang@ibp.ac.cn

Received 19 August 2016
Accepted 2 December 2016

Edited by N. Sträter, University of Leipzig, Germany

Keywords: Fun30; Snf2; structure; remodeller; ATPase.

PDB reference: C-terminal part of Fun30 ATPase domain, 5gn1

Supporting information: this article has supporting information at journals.iucr.org/f

Fun30 (Function unknown now 30) is a chromatin remodeller belonging to the Snf2 family. It has previously been reported to be a regulator of several cellular activities, including DNA repair, gene silencing and maintenance of chromatin structure. Here, the crystal structure of the Fun30 ATPase-C domain (the C-lobe of the ATPase domain) is reported at 1.95 Å resolution. Although the structure displays overall similarities to those of other Snf2 family members, a new structural module was found to be specific to the Fun30 subfamily. Fun30 ATPase-C was shown be monomeric in solution and showed no detectable affinity for dsDNA.

1. Introduction

The tightly packed structure of the chromosome is an obstacle to many cellular activities, including transcription, duplication and DNA repair. A subset of Snf2 family proteins act as remodellers to change the local structure of chromatin and facilitate the access of regulators to the DNA sequence. Fun30 was originally identified by whole-genome sequencing of budding yeast (Clark *et al.*, 1992), and was classified as a chromatin-remodelling enzyme (remodeller) based on sequence alignment (Flaus *et al.*, 2006). Consistent with the taxonomic identification, the function of Fun30 was reported to be confined to chromosome-associated activities such as chromosome stability, integrity and segregation (Ouspenski *et al.*, 1999). Specifically, recombinant Fun30 shows an ATPase activity that is stimulated by DNA and chromatin *in vitro*, and exhibits ATP-dependent chromatin-remodelling and histone dimer-exchange activity (Awad *et al.*, 2010). Additionally, Fun30 is involved in gene silencing (Neves-Costa *et al.*, 2009; Byeon *et al.*, 2013), point centromere function (Durand-Dubief *et al.*, 2012) and DNA double-strand break (DSB) repair (Chen *et al.*, 2012; Costelloe *et al.*, 2012). Fun30 is evolutionarily and functionally conserved in eukaryotes. Fft3 and SMARCAD1, the orthologues of Fun30 in fission yeast and human, respectively, are involved in heterochromatin structure maintenance (Strålfors *et al.*, 2011; Yu *et al.*, 2011; Steglich *et al.*, 2015; Rowbotham *et al.*, 2011) and DSB repair (Costelloe *et al.*, 2012).

Fun30 contains 1131 amino acids, with an ATPase domain located in the C-terminal part (residues 570–1131) as well as a region of unknown function (residues 1–570) at the N-terminus. The Fun30 ATPase domain possesses common characteristics of the Snf2 family proteins and is the structural basis for its chromatin-remodelling function (Awad *et al.*, 2010;

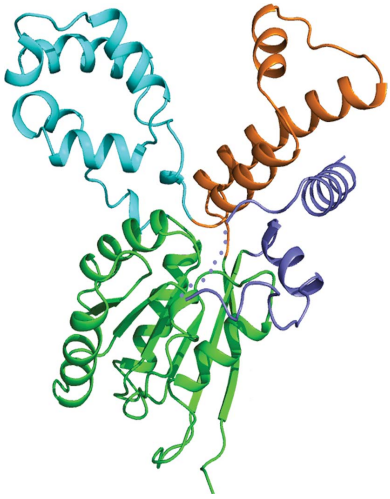

Flaus *et al.*, 2006). Snf2 enzymes, a subgroup of the helicase family, possess seven helicase-related motifs (I, Ia and II–VI) in the ATPase domain. The extra sequence blocks (blocks A–N), which are conserved only in the Snf2 family, differentiate the Snf2 family from other helicases (Flaus *et al.*, 2006). The ATPase domain, the central architectural component of Snf2 proteins, has been well studied biochemically, and several structures have been reported (Dürr *et al.*, 2005; Thomä *et al.*, 2005; Hauk *et al.*, 2010; Shaw *et al.*, 2008; Xia *et al.*, 2016). According to these structures, the ATPase domain is divided into two parts, ATPase-N and ATPase-C, which are connected by a linker. The former is the ATP-binding site and the latter participates in tracking along the DNA (Dürr *et al.*, 2005). In contrast to the high homology in sequence and global architecture of Snf2 proteins, the local regions between blocks C and K vary greatly, with various domain/motif insertions. These regions are therefore called major insertion sites (Flaus *et al.*, 2006). These insertions increase the structural variety of Snf2 enzymes, enabling them to fulfil diverse cellular activities.

The Snf2 family members are classified into 24 subfamilies based on the similarity in sequence in the ATPase domain. The Fun30 subfamily has a distant relationship to the other members. In this study, we determined the structure of Fun30 ATPase-C at 1.95 Å resolution. Structure comparison and sequence alignment with other Snf2 proteins revealed that insertion II, which is composed of five α-helices and two 3_{10}-helices, is specific to the Fun30 subfamily. Several biophysical approaches have been used to elucidate the oligomeric state of the ATPase-C domain of Fun30 and its DNA-binding properties.

Table 1
Macromolecule-production information.

The restriction-enzyme cleavage sites are underlined in the primers and the additional residues expressed by the vector are underlined in the amino-acid sequence.

Source organism	*S. cerevisiae*
DNA source	Genomic DNA
Forward primer	5′-GAGGATCCATGCCGCTATTAGCGCAAGAAGC-CA-3′
Reverse primer	5′-GCGCTCGAGTCATCATAAATTATATCCTCC-3′
Cloning vector	pET-21a
Expression vector	pET-21a
Expression host	*E. coli* Rosetta (DE3)
Complete amino-acid sequence of the construct produced	MASMTGGQQMGRGSMPLLAQEAITRAKTMMKPFI-LRRRKDQVLKHLPPKHTHIQYCELNAIQKKIY-DKEIQIVLEHKRMIKDGELPKDAKEKSKLQSS-SSKNLIMALRKASLHPLLFRNIYNDKIITKMS-DAILDEPAYAENGNKEYIKEDMSYMTDFELHK-LCCNFPNTLSKYQLHNDEWMQSGKIDALKKLL-KTIIVDKQEKVLIFSLFTQVLDILEMVLSTLD-YKFLRLDGSTQVNDRQLLIDKFYEDKDIPIFI-LSTKAGGFGINLVCANNVIIFDQSFNPHDDRQ-AADRAHRVGQTKEVNITTLITKDSIEEKIHQL-AKNKLALDSYISEDKKSQDVLESKVSDMLEDI-IYDELEHHHHHH

Table 2
Crystallization.

Method	Hanging-drop vapour diffusion
Temperature (K)	289
Protein concentration (mg ml^{-1})	10
Buffer composition of protein solution	25 m*M* HEPES pH 7.0, 150 m*M* NaCl
Composition of reservoir solution	0.1 *M* sodium malonate pH 5.0, 12% PEG 3350
Volume and ratio of drop	1 µl protein solution mixed with 1 µl reservoir solution
Volume of reservoir (µl)	500

2. Materials and methods

2.1. Macromolecule production

The DNA fragment coding for Fun30 ATPase-C (residues 780–1122) was amplified from the *Saccharomyces cerevisiae* genome and inserted into the pET-21a expression vector between BamHI and XhoI sites with a 6×His tag at the C-terminus. The recombinant plasmid was verified by DNA sequencing and then transformed into *Escherichia coli* Rosetta (DE3) cells for protein expression.

For large-scale expression, the *E. coli* cells were cultured in LB medium at 310 K. When the optical density (OD_{600}) of the cell cultures reached 0.8, the cultures were cooled to 289 K. Protein expression was induced by adding 0.3 m*M* isopropyl β-D-1-thiogalactopyranoside (IPTG). The cells were harvested 16 h later, resuspended in buffer *A* (20 m*M* Tris pH 8.0, 300 m*M* NaCl, 20 m*M* imidazole, 10% glycerol, 1 m*M* PMSF) and then disrupted by sonication. The bacterial cell lysate was centrifuged and the supernatant was applied onto an Ni–NTA column (GE Healthcare) pre-equilibrated with buffer *A*. The column was washed with buffer *B* (20 m*M* Tris pH 8.0, 300 m*M* NaCl, 50 m*M* imidazole, 10% glycerol) and eluted with buffer *C* (20 m*M* Tris pH 8.0, 300 m*M* NaCl, 300 m*M* imidazole, 10% glycerol). Samples were further purified by anion-exchange chromatography using a Resource S column (GE Healthcare). Elution was conducted with a linear gradient of NaCl concentration (0.08–1 *M*) in 25 m*M* HEPES pH 7.0 and the fractions were analyzed by SDS–PAGE. Fractions containing the target protein were pooled, concentrated and loaded onto a HiLoad Superdex 200 10/300 gel-filtration column pre-equilibrated with buffer *D* (25 m*M* HEPES pH 7.0, 150 m*M* NaCl). Fractions containing Fun30 were collected, concentrated and stored at 193 K. Macromolecule-production information is summarized in Table 1.

2.2. Crystallization

An initial crystallization screen was performed using the hanging-drop vapour-diffusion method at 289 K. Crystals were obtained using a reservoir solution consisting of 0.1 *M* sodium malonate pH 5.0, 12% PEG 3350. The crystals were soaked in a cryoprotectant consisting of 20% PEG 3350 in the reservoir and then flash-cooled in liquid nitrogen. Crystallization information is summarized in Table 2.

2.3. Data collection and processing

The X-ray diffraction data were collected on the BL-1A beamline at the Photon Factory (PF), Tsukuba, Japan. The data set was processed with *HKL*-2000 (Otwinowski & Minor,

Table 3
Data collection and processing.

Values in parentheses are for the outer shell.

Diffraction source	BL-1A, PF
Wavelength (Å)	1.1000
Temperature (K)	100
Detector	PILATUS 2M-F
Crystal-to-detector distance (mm)	177.61
Rotation range per image (°)	1.0
Total rotation range (°)	360
Exposure time per image (s)	0.2
Space group	*C*2
a, *b*, *c* (Å)	114.43, 118.39, 111.58
α, β, γ (°)	90, 107.28, 90
Mosaicity (°)	0.3
Resolution range (Å)	50–1.95 (1.98–1.95)
Total No. of reflections	697715
No. of unique reflections	103556
Completeness (%)	100.0 (100.0)
Multiplicity	6.7 (6.8)
$\langle I/\sigma(I)\rangle$	20.73 (2.13)
$R_{\rm meas}$	0.089 (0.698)
Overall *B* factor from Wilson plot (Å^2)	25.88

Table 4
Structure solution and refinement.

Values in parentheses are for the outer shell.

Resolution range (Å)	35.47–1.95 (2.02–1.95)
Completeness (%)	100.0
No. of reflections, working set	103156 (10276)
No. of reflections, test set	1993 (198)
Final $R_{\rm cryst}$	0.184 (0.228)
Final $R_{\rm free}$	0.214 (0.265)
No. of non-H atoms	
Protein	10165
Water	1243
R.m.s. deviations	
Bonds (Å)	0.011
Angles (°)	1.04
Average *B* factors (Å^2)	
Overall	30.58
Protein	31.43
Water	37.79
Ramachandran plot	
Most favoured (%)	98.5
Allowed (%)	1.5

1997). Data-collection and processing statistics are given in Table 3.

2.4. Structure solution and refinement

The initial phase was obtained by molecular replacement with *Phaser* (McCoy *et al.*, 2007) as implemented in *CCP*4 (Winn *et al.*, 2011). The structure of Chd1 (PDB entry 3mwy; Hauk *et al.*, 2010) was modified for use as a search model. The initial model was built with *AutoBuild* in *PHENIX* (Adams *et al.*, 2010) and then modified and refined using alternate rounds of *Coot* (Emsley & Cowtan, 2004) and *phenix.refine* (Afonine *et al.*, 2012). The final structure was refined to 1.95 Å resolution. Details of the refinement statistics are shown in Table 4. Atomic coordinates and structure factors have been deposited in the Protein Data Bank (http://www.pdb.org) as entry 5gn1. Structural figures were prepared with *PyMOL* (v.1.5; Schrödinger).

2.5. Size-exclusion chromatography coupled with light scattering

We measured the mass of Fun30 ATPase-C in solution using a Wyatt Eclipse 3 separation system combined with a static light-scattering detector (DAWN HELEOS II, Wyatt) and a differential refractive-index detector (Optilab rEX detector, Wyatt). Protein sample (50 µl at a concentration of 1.4 mg ml^{-1}) was injected onto a Superdex 75 10/300 GL column (GE Healthcare) with column buffer consisting of 20 m*M* HEPES pH 7.5, 150 m*M* NaCl. Data were analyzed with *ASTRA* 6.1 (Wyatt)

2.6. Analytic ultracentrifugation

Sedimentation-velocity experiments were performed using a Beckman Coulter ProteomeLab XL-I analytical ultracentrifuge equipped with an An-60 Ti rotor (four holes) and conventional double-sector aluminium centrepieces of 12 mm optical path length loaded with 380 µl sample and 400 µl buffer (20 m*M* Tris pH 8.0, 200 m*M* NaCl). The experiment was carried out at 20°C and 50 000 rev min^{-1} using an absorption optical scanner (ABS) at 280 nm. Data were analyzed using *SEDFIT* (https://sedfitsedphat.nibib.nih.gov/software) and the continuous $c(s)$ distribution model.

2.7. Electrophoretic mobility shift assay (EMSA)

The oligonucleotides 5′-6-FAM-AAAAAAATTGCCGA-AGACGAAAAAA-3′ and 5′-TTTTTTTCGTCTTCGGCA-ATTTTTT-3′ were synthesized and annealed to form the substrate dsDNA. The 6-FAM label was added at the 5′ end for detection. 1 µ*M* dsDNA was pre-incubated with Fun30 ATPase-C (residues 780–1122) or ATPase-N (residues 572–794) at concentrations ranging from 0.5 to 10 µ*M*. Fun30 ATPase-N was expressed in *E. coli* and purified using Ni–NTA column and size-exclusion chromatography. The EMSA binding buffer consisted of 25 m*M* HEPES pH 7.5, 150 m*M* NaCl, 2 m*M* DTT. After incubation at 289 K for 30 min, the reaction products were loaded onto a 6% nondenaturing polyacrylamide gel and resolved by electrophoresis at 277 K and 10 V cm^{-1} in 0.5× TBE buffer. Gels were visualized using a Typhoon FLA 7000.

3. Results and discussion

3.1. Overall structure of Fun30 ATPase-C

A Fun30 fragment spanning residues 780–1122 was expressed, purified and crystallized. The crystals grew to full size after 2 d and diffracted to about 1.95 Å resolution at a synchrotron (Table 1). Our construct includes the ATPase-C domain and the linker between the two lobes, whereas the linker (residues 780–808) is not visible in the electron-density map. The crystal belonged to space group *C*2 with four molecules per asymmetric unit, and the structure was determined using the molecular-replacement method with the structure of the Chd1 ATPase-C domain (PDB entry 3mwy) as the initial search model. Superimposition of the four

molecules in the asymmetric unit shows little difference, with a root-mean-square deviation (r.m.s.d.) of about 0.5 Å.

As shown in Fig. 1, the overall structure of Fun30 ATPase-C shows a cloverleaf pattern and is composed of four parts: a conserved RecA-like fold as the core structure (residues 814–820 and 948–1075), an Snf2-specific helix insertion (insertion I; residues 821–874), a nonconserved helix-bundle insertion (insertion II; residues 875–947) and a C-terminal extension (CTE; residues 1076–1122). The RecA-like fold, which includes motifs IV, V and VI and blocks B, K, D and L, forms an α/β structure characterized by a central β-sheet flanked by five α-helices (Fig. 1*c*). Residue Arg1058, also called the arginine finger, is conserved in the helicase family and participates in the formation of the catalytic centre. Insertion I containing blocks C and J is composed of three tandem α-helices, two of which are almost antiparallel, with the middle helix nearly perpendicular to the other two helices. Insertion II between blocks C and K is composed of five α-helices and

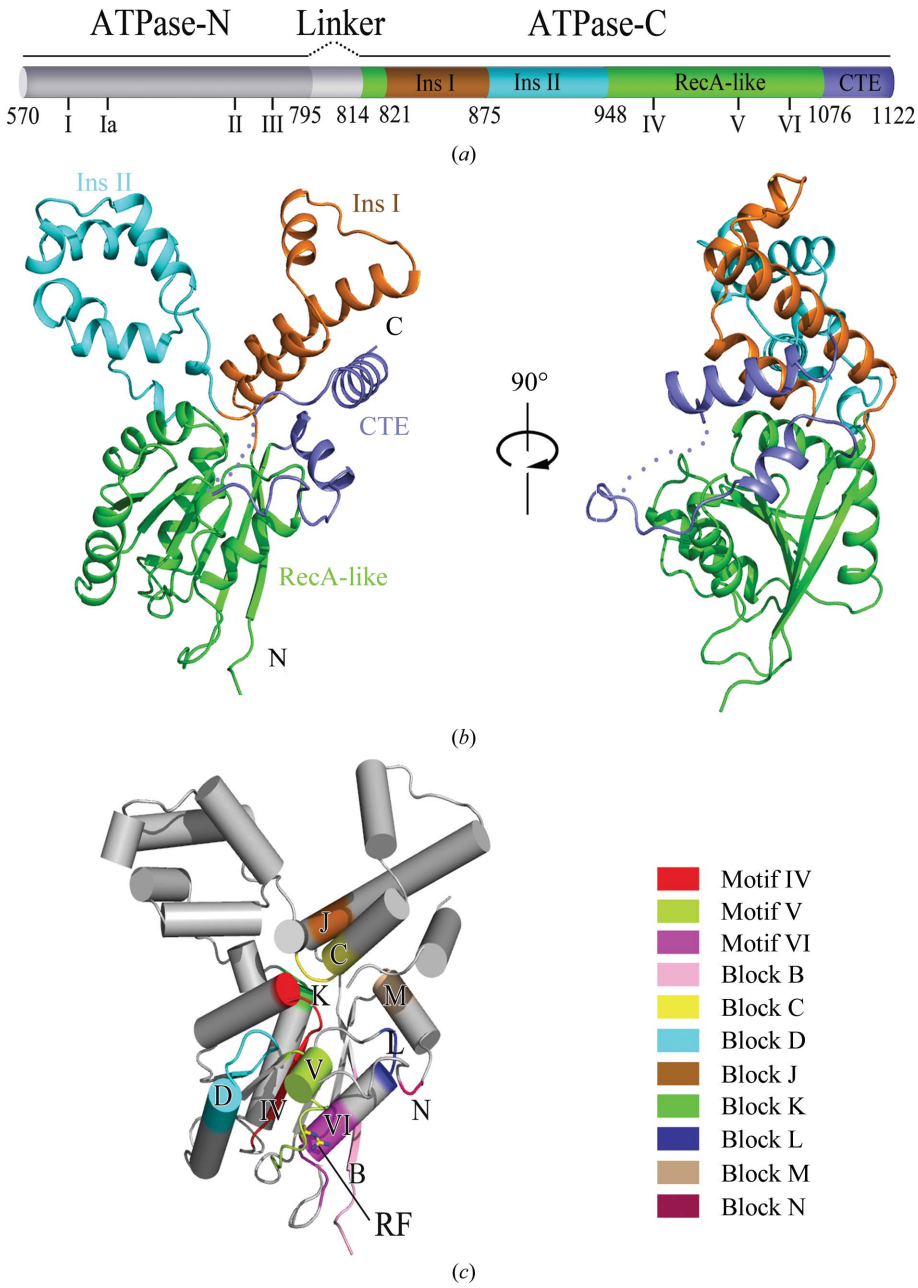

Figure 1
Overview of the structure of Fun30 ATPase-C. (*a*) Schematic representation of the Fun30 ATPase motor organization. The ATPase-N is shown in grey and the ATPase-C is in colour. The RecA-like fold, insertion I (Ins I), insertion II (Ins II) and the CTE are depicted in green, orange, cyan and blue, respectively. The locations of the conserved helicase-related motifs I–VI are marked below the cartoon diagram. (*b*) Cartoon representation of Fun30 ATPase-C. The colours of the different segments are the same as in (*a*). The loop in the CTE which is not modelled is displayed with dots. (*c*) The conserved motifs and blocks mapped onto Fun30 ATPase-C. Motif IV (residues 968–976), motif V (residues 1024–1034), motif VI (residues 1054–1061), block B (residues 810–815), block C (residues 871–878), block D (residues 995–1005), block J (residues 826–830), block K (residues 948–950), block L (residues 1047–1049), block M (residues 1079–1082) and block N (residues 1090–1091) are coloured according to the legend. Residue Arg1058, the conserved arginine finger in motif IV, is shown as a stick model.

two 3_{10}-helices. This inserted helix bundle is not conserved in the whole Snf2 family, but shows higher conservation within its subfamily (Fig. 2*e*). The CTE packed in the cleft between insertion I and the RecA-like fold contains blocks M and N, and comprises two α-helices linked by a 23-residue loop. Part of the loop (residues 1098–1103) could not be modelled owing to its high flexibility.

3.2. Structural comparison between Fun30 and its homologues

To identify the structural features of Fun30 ATPase-C, we superposed it on four Snf2 enzymes, SSO1653 (PDB entry 1z6a; Dürr *et al.*, 2005), Rad54 (PDB entry 1z3i; Thomä *et al.*, 2005), Chd1 (PDB entry 3mwy; Hauk *et al.*, 2010) and Snf2 (PDB entry 5hzr; Xia *et al.*, 2016), that belong to distinct subfamilies. As shown in Figs. 2(*a*)–2(*d*), the greatest differences were found to be located in the insertion regions. Insertion I in Fun30 is composed of three helices, whereas its counterparts in the other four proteins consist of two helices linked by a loop. In addition, the structure of insertion II in Fun30 is much larger and more complex than the others. The sequence of the middle helix of Fun30 insertion I is not conserved according to sequence alignment (data not shown), whereas insertion II is highly conserved in the Fun30 subfamily (Fig. 2*e*). Therefore, insertion II seems to be a hallmark of the Fun30 subfamily. The insertions at the major insertion site usually confer specific functions on Snf2 proteins. For example, the insertion of a RING domain into the ATPase domain of Rad5/Rad16 subfamily enables them to be a component of the E3 ubiquitin ligase in addition to a remodeller (Parker & Ulrich, 2009; Gillette *et al.*, 2006). Thus, it is reasonable to speculate that insertion II may be related to certain conserved functions of the Fun30 subfamily. Futher biochemical data are needed to elucidate the function of the Fun30 insertion regions.

3.3. Fun30 ATPase-C is in a monomeric state

As shown in Fig. 3(*a*), our structural model contains four molecules arranged in an asymmetric unit; however, the interactions among these molecules are so weak that this arrangement is most likely to be a result of crystal packing. We also noticed that the molecules from two neighbouring asymmetric units form tight interactions (Fig. 3*a*). Insertion I and the CTE of one molecule generate extensive hydrogen bonds with insertions I and II of the other molecule (Fig. 3*b*). Furthermore, the area of the interface, as analyzed by the *PISA* server (Krissinel & Henrick, 2007), is 1933.1 Å^2. The large area of the interface supports the formation of a dimer.

However, during gel filtration using a Superdex 200 10/300 column the protein eluted at a volume of 16.2 ml, with an apparent molecular mass of about 40 kDa (Fig. 3*c*), which corresponds to an ATPase-C monomer. In order to investigate the oligomeric state of Fun30 ATPase-C more precisely, we utilized size-exclusion chromatography coupled with static light scattering and analytical ultracentrifugation. The molecular weight of Fun30 ATPase-C was determined to be about 34 kDa by those two methods (Fig. 3*d* and 3*e*). The results both agree with the weight of a monomer. The measured molecular mass may be smaller than the calculated mass owing to a slight degradation of the N-terminus of the recombinant expressed fragment. Therefore, we propose that Fun30 ATPase-C is a monomer in solution but forms a dimer in crystal packing.

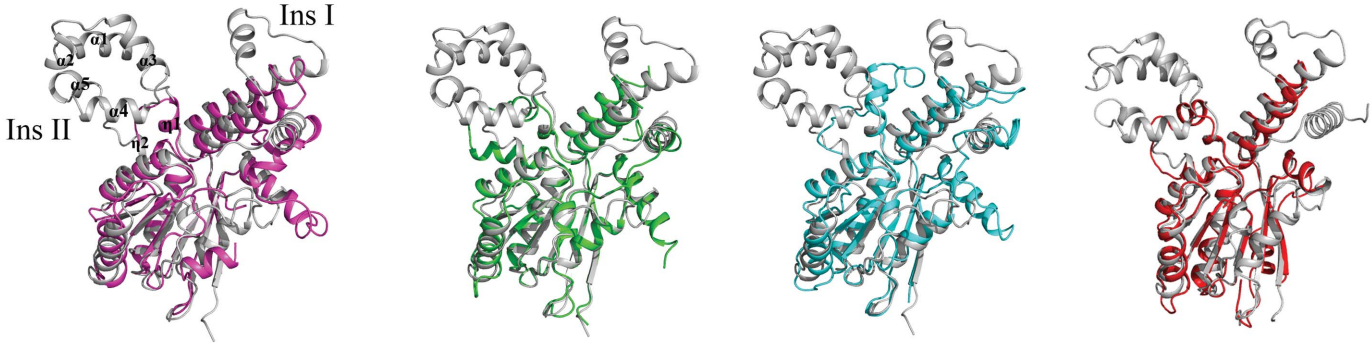

Figure 2
Comparison of Fun30 ATPase-C with its homologues. (*a*–*d*) Superposition of Fun30 ATPase-C (grey) on SSO1653 (magenta), Chd1 (green), Rad54 (cyan) and Snf2 (red). The comparison highlights the differences in the insertion I and insertion II regions. (*e*) Sequence alignment of insertion II in the Fun30 subfamily, including Fft3 from *Schizosaccharomyces pombe* (*Sp*), CG5899 from *Drosophila melanogaster* (*Dm*), M03C11.8 from *Caenorhabditis elegans* (*Ce*), Etl1 from mouse (*Mm*) and SMARCAD1 from human (*Hs*). Conserved regions are shown in blue boxes. Highly conserved residues are in white and shaded red; moderately conserved residues are in red. Sequence alignment was performed using *ESPript* (Robert & Gouet, 2014).

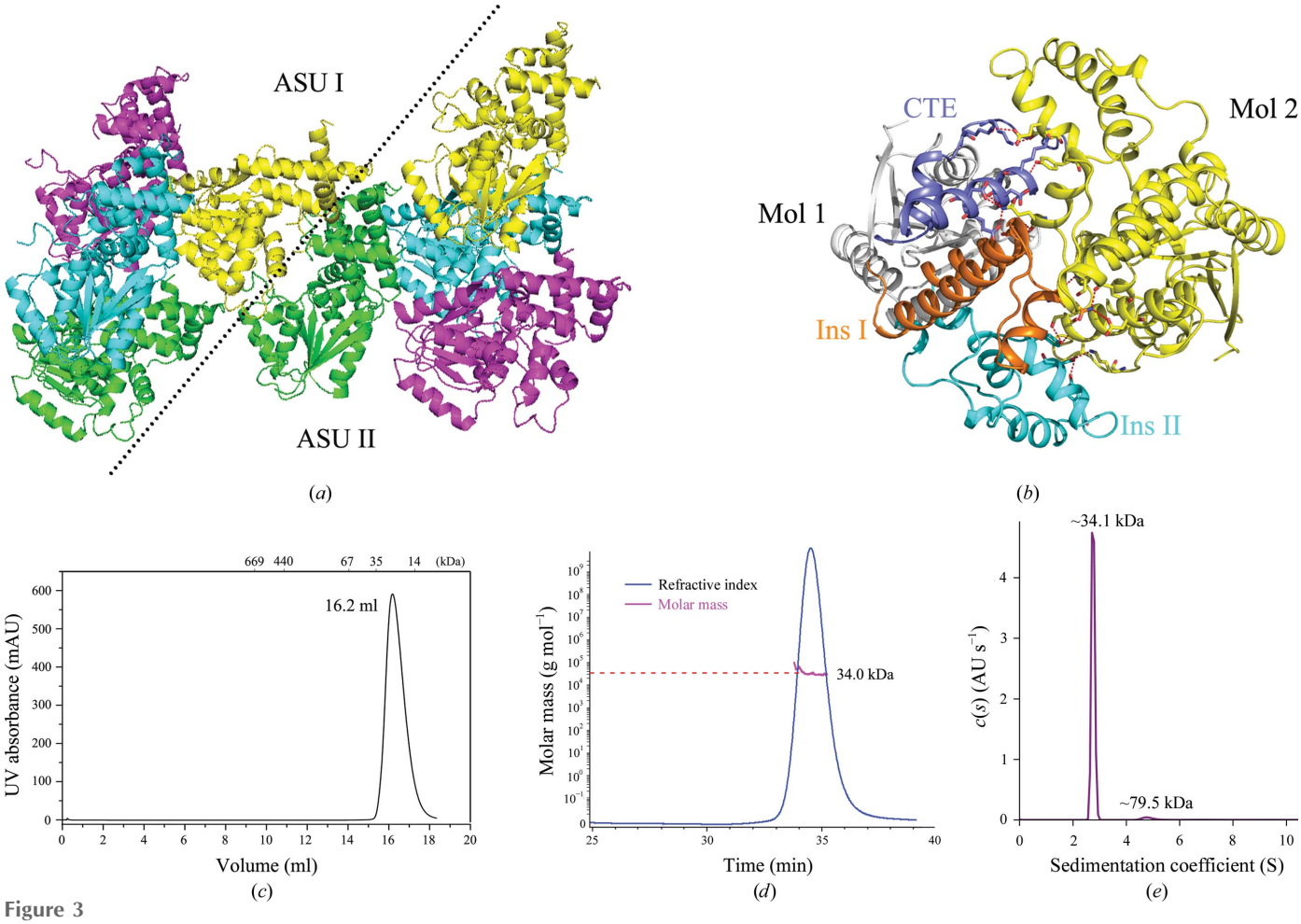

Figure 3
Fun30 ATPase-C is a monomer in solution. (*a*) Monomers from neighbouring asymmetric units (ASUs) form tight interactions. The four monomers in an asymmetric unit are in different colours. (*b*) The interface of the dimer in the crystal. The CTE (blue), Ins I (orange) and Ins II (cyan) of one monomer interact with the other monomer (yellow). Hydrogen bonds are shown as red dashed lines. (*c*) Size-exclusion chromatogram of Fun30 ATPase-C. The molecular masses of the protein standards are indicated at the top. (*d*) The mass of Fun30 ATPase-C in solution is about 34.0 kDa, as measured by static light scattering, which corresponds to a monomeric configuration. (*e*) Analytical ultracentrifugation of Fun30 ATPase-C demonstrates that 95.8% of the total protein, with a molecular mass of about 34.1 kDa, is a monomer. Only 2.6% of the sample shows a molecular mass of 79.5 kDa, which may be an impurity.

Since full-length Fun30 has been reported to form a homodimer *in vitro* and *in vivo* (Awad *et al.*, 2010), we speculated that certain sequences outside Fun30 ATPase-C are responsible for the dimerization of Fun30. This speculation is supported by our research on Fun30 ATPase-N, which exhibits both monomeric and dimeric states in solution according to the results of analytical ultracentrifugation (Supplementary Fig. S1).

3.4. Fun30 ATPase-C has little affinity for dsDNA

The ATPase domain of Snf2 family proteins is not only the catalytic core of ATP hydrolysis, but also the site for DNA binding. In the structure of the SSO1653–dsDNA complex (PDB entry 1z63) the DNA strands lie in the cleft between the ATPase-N and ATPase-C domains. The ATPase-N domain of SSO1653 displays comparable affinity for DNA as that of the full ATPase motor, whereas the ATPase-C domain by itself shows little affinity for DNA (Dürr *et al.*, 2005). Since Fun30 has previously been reported to have affinity for dsDNA (Awad *et al.*, 2010), we tested whether Fun30 ATPase-C retained the affinity for dsDNA. The results of EMSA showed that Fun30 ATPase-C alone was unable to bind dsDNA, whereas the ATPase-N domain bound dsDNA to form a supershift on native PAGE (Fig. 4). This result indicated that Fun30, just like SSO1653, uses the ATPase-N domain as the main site to interact with DNA. Fun30 may adopt a similar way of binding DNA as other Snf2 proteins.

4. Conclusions

In summary, we determined the crystal structure of the C-terminal part of the Fun30 ATPase domain at 1.95 Å resolution. This is the first structural report from the Fun30 subfamily to date. Sequential and structural comparison of Fun30 ATPase-C with its homologues demonstrated that Fun30 ATPase-C has the same conserved motifs and the same structural fold as its homologues, but possesses a helix-bundle

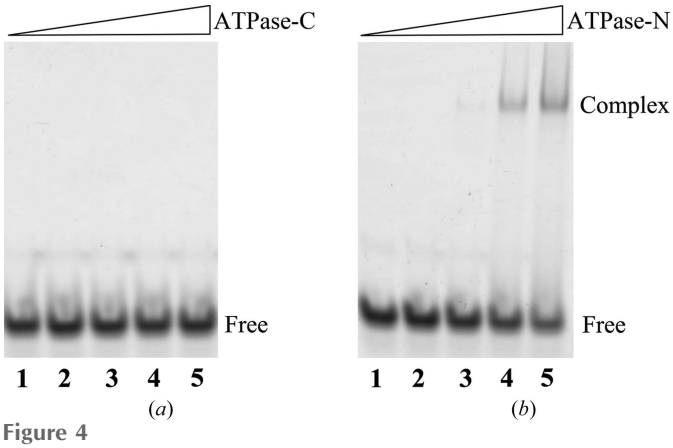

Figure 4
Fun30 ATPase-C has little DNA-binding affinity. The DNA-binding abilities of ATPase-C (*a*) and ATPase-N (*b*) were tested by EMSA; lane 1 shows the dsDNA substrate as a control and lanes 2–5 contain samples with increasing protein concentrations, resulting in final protein:DNA molar ratios of 0.5, 2, 5 and 10, respectively.

insertion that is specific to the Fun30 subfamily. Moreover, we showed that Fun30 ATPase-C is monomeric in solution and has little affinity for dsDNA. These results will aid in future biochemical analyses of Fun30, as well as other members of the Fun30 subfamily.

Acknowledgements

We thank the staff at the BL-1A beamline, Photon Factory, Tsukuba, Japan for technical assistance during data collection. This work was supported by the Strategic Priority Research Program (XDB08010301).

References

Adams, P. D. *et al.* (2010). *Acta Cryst.* D**66**, 213–221.
Afonine, P. V., Grosse-Kunstleve, R. W., Echols, N., Headd, J. J., Moriarty, N. W., Mustyakimov, M., Terwilliger, T. C., Urzhumtsev, A., Zwart, P. H. & Adams, P. D. (2012). *Acta Cryst.* D**68**, 352–367.
Awad, S., Ryan, D., Prochasson, P., Owen-Hughes, T. & Hassan, A. H. (2010). *J. Biol. Chem.* **285**, 9477–9484.
Byeon, B., Wang, W., Barski, A., Ranallo, R. T., Bao, K., Schones, D. E., Zhao, K., Wu, C. & Wu, W.-H. (2013). *J. Biol. Chem.* **288**, 23182–23193.
Chen, X., Cui, D., Papusha, A., Zhang, X., Chu, C.-D., Tang, J., Chen, K., Pan, X. & Ira, G. (2012). *Nature (London)*, **489**, 576–580.
Clark, M. W., Zhong, W. W., Keng, T., Storms, R. K., Barton, A., Kaback, D. B. & Bussey, H. (1992). *Yeast*, **8**, 133–145.
Costelloe, T., Louge, R., Tomimatsu, N., Mukherjee, B., Martini, E., Khadaroo, B., Dubois, K., Wiegant, W. W., Thierry, A., Burma, S., van Attikum, H. & Llorente, B. (2012). *Nature (London)*, **489**, 581–584.
Durand-Dubief, M., Will, W. R., Petrini, E., Theodorou, D., Harris, R. R., Crawford, M. R., Paszkiewicz, K., Krueger, F., Correra, R. M., Vetter, A. T., Miller, J. R., Kent, N. A. & Varga-Weisz, P. (2012). *PLoS Genet.* **8**, e1002974.
Dürr, H., Körner, C., Müller, M., Hickmann, V. & Hopfner, K. P. (2005). *Cell*, **121**, 363–373.
Emsley, P. & Cowtan, K. (2004). *Acta Cryst.* D**60**, 2126–2132.
Flaus, A., Martin, D. M., Barton, G. J. & Owen-Hughes, T. (2006). *Nucleic Acids Res.* **34**, 2887–2905.
Gillette, T. G., Yu, S., Zhou, Z., Waters, R., Johnston, S. A. & Reed, S. H. (2006). *EMBO J.* **25**, 2529–2538.
Hauk, G., McKnight, J. N., Nodelman, I. M. & Bowman, G. D. (2010). *Mol. Cell*, **39**, 711–723.
Krissinel, E. & Henrick, K. (2007). *J. Mol. Biol.* **372**, 774–797.
McCoy, A. J., Grosse-Kunstleve, R. W., Adams, P. D., Winn, M. D., Storoni, L. C. & Read, R. J. (2007). *J. Appl. Cryst.* **40**, 658–674.
Neves-Costa, A., Will, W. R., Vetter, A. T., Miller, J. R. & Varga-Weisz, P. (2009). *PLoS One*, **4**, e8111.
Otwinowski, Z. & Minor, W. (1997). *Method Enzymol.* **276**, 307–326.
Ouspenski, I. I., Elledge, S. J. & Brinkley, B. R. (1999). *Nucleic Acids Res.* **27**, 3001–3008.
Parker, J. L. & Ulrich, H. D. (2009). *EMBO J.* **28**, 3657–3666.
Robert, X. & Gouet, P. (2014). *Nucleic Acids Res.* **42**, W320–W324.
Rowbotham, S. P., Barki, L., Neves-Costa, A., Santos, F., Dean, W., Hawkes, N., Choudhary, P., Will, W. R., Webster, J., Oxley, D., Green, C. M., Varga-Weisz, P. & Mermoud, J. E. (2011). *Mol. Cell*, **42**, 285–296.
Shaw, G., Gan, J. H., Zhou, Y. N., Zhi, H. J., Subburaman, P., Zhang, R. G., Joachimiak, A., Jin, D. J. & Ji, X. H. (2008). *Structure*, **16**, 1417–1427.
Steglich, B., Strålfors, A., Khorosjutina, O., Persson, J., Smialowska, A., Javerzat, J. P. & Ekwall, K. (2015). *PLoS Genet.* **11**, e1005101.
Strålfors, A., Walfridsson, J., Bhuiyan, H. & Ekwall, K. (2011). *PLoS Genet.* **7**, e1001334.
Thomä, N. H., Czyzewski, B. K., Alexeev, A. A., Mazin, A. V., Kowalczykowski, S. C. & Pavletich, N. P. (2005). *Nature Struct. Mol. Biol.* **12**, 350–356.
Winn, M. D. *et al.* (2011). *Acta Cryst.* D**67**, 235–242.
Xia, X., Liu, X., Li, T., Fang, X. & Chen, Z. (2016). *Nature Struct. Mol. Biol.* **23**, 722–729.
Yu, Q., Zhang, X. & Bi, X. (2011). *J. Biol. Chem.* **286**, 14659–14669.